Geomechanics and Engineering, *Vol. 23, No. 4 (2020) 365-379*
DOI: https://doi.org/10.12989/gae.2020.23.4.365

Mitigation of liquefaction-induced uplift of underground structures by soil replacement methods

Priya Beena Sudevan[a], A. Boominathan* and Subhadeep Banerjee[b]

Department of Civil Engineering, Indian Institute of Technology, Madras, Chennai 600036, India

(Received July 29, 2019, Revised November 1, 2020, Accepted November 5, 2020)

Abstract. One of the leading causes for the damage of various underground structures during an earthquake is soil liquefaction, and among this liquefaction-induced uplift of these structures is a major concern. In this study, finite-difference modelling is carried out to study the liquefaction-induced uplift of an underground structure of 5 m diameter (D) with and without the replacement of the in-situ fine sand around the structure with the coarse sand. Soil replacements are carried out by three methods: replacement of soil above the structure, around the structure, and below the structure. The soil behaviour is represented using the elastic-perfectly plastic Mohr-Coulomb model, where the pore pressures were computed using Finn-Byrne formulation. The predicted pore pressure and uplift of the structure due to sinusoidal input motion were validated with the centrifuge tests reported in the literature. Based on numerical studies, an empirical equation is developed for the determination of liquefaction-induced maximum uplift of the underground structure without replacement of the in-situ sand. It is found that the replacement of soil around the structure with 2D width and spacing of D can reduce the maximum uplift by 50%.

Keywords: finite difference modelling; underground structure; liquefaction-induced uplift; pore pressure response; mitigation; replacement of soil

1. Introduction

Due to the fast expansion of land use, the majority of the newly built structures, including roads, metro tunnels, and pipelines, are going underground. These structures are essential for civic services and managing good quality of life. In general, underground structures are exposed to various natural and manmade challenges (Foriero and Ladanyi 1994, Koseki *et al*. 1997a, Nobahar *et al*. 2007, Huange *et al*. 2013, Williams *et al*. 2013, Roberta *et al*. 2016). However, they are more prone to damages when subjected to strong ground motions. In general, numerous factors influence the response of underground structures subjected to earthquake loading (Chou *et al*. 2001, Aydingun and Adalier 2003, Arango 2008, Yu *et al*. 2017). Among these factors, the damages caused due to the floatation of structures buried within liquefiable soil after ground shaking is most detrimental. Such severe damages in liquefiable soil were observed after numerous earthquake events including the 1934 Nepal-Bihar earthquake (Murty and Malik 2008), 1964 Niigata earthquake (Koseki *et al*. 1997a), 2007 Niigataken-Chuetsu-Oki earthquake (Onoue and Toyota 2008, Tanaka *et al*. 2011), 2010 Canterbury earthquake (Sherson *et al*. 2015) and 2011 Tohoku Pacific earthquake (Tokimatsu and Katsumata 2012).

In the past, research works on the soil-structure interaction, and the behaviour of various underground structures with and without seismic effects have been done extensively (Nagy *et al*. 2010, Chou *et al*. 2011, Chakraborty and Kumar 2013, Chian and Madabhushi 2013, Mahdi and Katebi 2015, Emirler *et al*. 2016, Robert and Thusyanthan 2016, Fabozzi *et al*. 2017, Singh et al. 2018, Yigit *et al*. 2018, Yatsumoto et al. 2019). Researchers have conducted studies to investigate the uplift mechanism of underground structures buried in liquefiable soil, which are subjected to earthquake loading (Koseki *et al*. 1997b, Ling *et al*. 2003, Ling *et al*. 2008, Chou *et al*. 2011, Chian and Madabhushi 2012, Liu 2012, Bao *et al*. 2017, Castiglia *et al*. 2018, Stringer and Madabhushi 2007, Sudevan *et al*. 2018, Sudevan *et al*. 2020). Koseki *et al*. (1997b) were one of the first to point out that the uplift of the underground structure during liquefaction is due to the lateral deformation of the soil and the movement of the pore fluid to the base of the structure. In the last few decades, researchers have conducted experimental (Ling *et al*. 2003, Yang *et al*. 2004, Tobita *et al*. 2011, Kang *et al*. 2014, Watanabe *et al*. 2016) and numerical (Liu and Song 2006, Ling *et al*. 2008, Liu 2012, Madabhushi and Madabhushi 2015, Bao *et al*. 2017) studies to understand the complete uplift behaviour of the underground structure subjected to seismic motion. These studies show that underground structures suffered several damages after floatation due to liquefaction. The primary reasons for underground structure floatation are high excess pore water pressure and input acceleration (Chian *et al*. 2014, Azadi and Hosseini *et al*. 2016a, Singh *et al*. 2018, Sudevan *et al*. 2020). Some other studies indicate that these uplifts are also dependent on the embedment depth of the structure, the depth of liquefiable soil below the structure, friction angle of the soil and

*Corresponding author, Professor
E-mail: boomi@iitm.ac.in
[a]Research Scholar
[b]Associate Professor

ISSN: 2005-307X (Print), 2092-6219 (Online)

characteristics of seismic loading (Azadi and Hosseini 2010b, Tobita *et al*. 2011, Yang and Wang 2012, Watanabe *et al*. 2016).

The mitigation of the liquefaction-induced uplift of various underground structures is critical for their optimal performance. There are many traditional techniques to prevent liquefaction of the soil which includes the soil improvement by densification (Modoni *et al*. 2018, Olarte *et al*. 2018, Mele *et al*. 2019), grouting (Ishii *et al*. 2013, Madoni *et al*. 2019), and dewatering (Yegin *et al*. 2007, Mitsuji 2008). However, research works on the mitigation of liquefaction-induced uplift is comparatively fewer. In the available works, two techniques were commonly used to reduce the displacement of the structure due to liquefaction of the soil: i) reducing the pore water accumulation around the structure (Tanaka *et al*. 1995, Olarte *et al*. 2018), and ii) accelerated dissipation of pore water from the vicinity of the structure (Adalier *et al*. 2003, Orense *et al*. 2003, Otsubo *et al*. 2016a, Otsubo *et al*. 2016b, Paramasivam *et al*. 2018). Other methods for mitigating the liquefaction-induced uplift includes providing barriers around the structures to prevent the lateral movement of the soil near the structure (Yoshimi 1998, Yasuda *et al*. 2004, Liu and Song 2006) and stabilising using some weight above the structure (Taeseri *et al*. 2016, Castiglia *et al*. 2017). More recently, Castiglia *et al*. (2019) used geogrids to effectively stabilise the liquefaction-induced uplift of a buried onshore pipeline structure.

The method of densification by compaction restricts the movement of pore water from the free field to the improved region and thereby, it enables mitigation of underground structures. Tanaka *et al*. (1995), from their experimental studies, proposed a design procedure to determine the area of densification required for effective mitigation of liquefaction of sand. The effect of the relative density of the soil was studied by Tobita *et al*. (2011). They reported a large structural uplift in the case of loose sand, which reduced slightly with an increase in the relative density of soil. In recent research work, Olarte *et al*. (2018) utilised the densification of soil to minimise the settlement of framed structures on liquefiable soil effectively.

Few researchers have also investigated the effect of accelerated drainage around the structure by replacing the problematic soil with more permeable soil (Miyajima *et al*. 1992, Orense *et al*. 2003, Yang *et al*. 2004, Otsubo *et al*. 2016b, Mahmoud *et al*. 2020). The possible benefits of this replacement of soil are that it accelerates the dissipation of pore water from the vicinity of the structure, and the replaced soil act as a stiffer material around the structure. The centrifuge shake table experiments carried out by Brennan and Madabhushi (2002) indicated that the gravel drains dissipated the pore pressure more quickly because of the shorter drainage path in the improved region. Adalier *et al*. (2003), from their centrifuge study, concluded that the combined effect of the densified wall and gravel drain on both sides of the structure provided a suitable mitigation design against the uplift of the buried structure. Orense *et al*. (2003) highlighted the effectiveness of crushed stones, without sand and fines content, as the drain material to reduce the displacement of various underground structures due to liquefaction of the soil. Otsubo *et al*. (2016b) studied the effect of different recyclable materials for mitigating the uplift of underground structures within liquefiable soil. They reported that, among these materials, crushed glass was most effective due to its higher permeability. Mahmoud *et al*. (2020) reported that the combined use of gravel drains near the structure and an impermeable layer below the structure effectively reduced the liquefaction-induced uplift of underground structures.

However, the mitigation of liquefaction-induced uplift of underground structures using the replacement method and the corresponding optimum parameters are scarcely investigated in the open literature. The replacement method is an easily employable mitigation method, and hence, it needs to be comprehensively investigated. In this work, a numerical study of uplift mitigation of the underground structure by the replacement of in-situ fine sand with coarse sand, along the length of the structure, is developed using a finite difference code, FLAC3D (Itasca consulting group 2012). The effectiveness of this method is highlighted and compared in terms of the pore pressure response developed at different levels within the model. The model also predicts the resulting liquefaction-induced uplift displacement of the structure. In addition to that, studies on the continuous replacement and replacement with regular intervals between the replaced areas are carried out.

2. Description of the problem studied

In this work, a typical hollow underground structure of diameter 5 m of concrete material embedded within a thick homogeneous sand deposit overlying the bedrock is considered. The sand considered in this study is the poorly graded Houston fine sand (Chian and Madabhushi 2013). The depth of embedment of the underground structure, h, is measured from the ground surface to the springing level of the structure for three cases: 1.1, 1.3, and 1.5 times the diameter of the underground structure (D), as shown in Fig. 1. The groundwater table is considered to the ground surface. The relative density of the sand (D_r) is varied from 45% to 65%. The experimental data from a large scale centrifuge study on the uplift response of an underground structure buried within a liquefiable soil, conducted by Chian and Madabhushi (2013), was chosen for the numerical simulation in the present study, and its geometric layout is shown in Fig. 1. The prototype dimensions were modelled using a 10 m diameter beam centrifuge at Cambridge University. The experimental model consists of a 240 mm thick homogenous Houston sand in an aluminium window box container. A hollow circular structure of 75 mm diameter with closed-ends was buried at different depths (1.1D, 1.5D) in a fully saturated soil medium. The model was spun at a centrifuge acceleration of 100 g while excited horizontally at the base.

The in-situ sand near the structure is replaced using coarse sand to mitigate the liquefaction-induced uplift of the underground structure. The coarse sand considered in the present study is Fraction B sand. A continuous replacement of in-situ sand of 2D width (measured perpendicular to the axis of the structure) is considered in the present study.

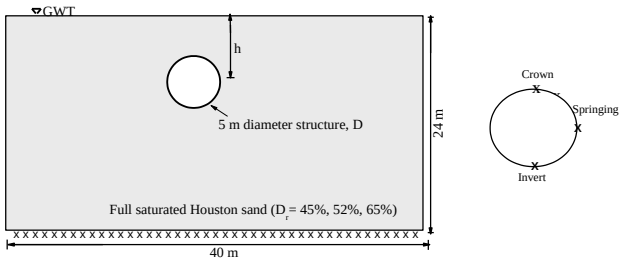

Fig. 1 Schematic view of present study model

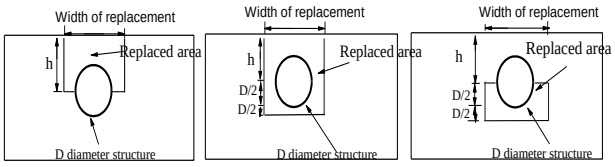

Fig. 2 Schematic view of the model with the replacement method

Three schemes of replacement methods are considered, and the geometric layout is shown in Fig. 2. In replacement method 1, the in-situ sand till the springing level of the structure (depth = h) is replaced by coarse sand, and in replacement method 2, the in-situ sand around the structure (depth = h+D) is replaced by coarse sand. In replacement method 3, the in-situ sand below the springing level (depth = D) of the structure is replaced by coarse sand. Apart from the continuous replacement of the in-situ sand along the direction of the structure, replacement of the in-situ sand with regular intervals of D and 2D spacing along the direction of the structure were also adopted.

3. Finite difference modelling

In the present study, numerical modelling of liquefaction-induced uplift of an underground structure with and without replacement of in-situ fine sand around the structure with coarse sand is carried out using finite difference code, FLAC3D (Itasca Consulting Group 2012).

In the numerical model, Cauchy's equation of motion (as represented in Eq. (1)) is used to estimate the stress and deformation within the continuum body.

$$\frac{\partial \sigma_{ij}}{\partial x_i} + \rho b_i = \rho \frac{\partial \upsilon_i}{\partial t} \tag{1}$$

where, σ_{ij} is the stress tensor, b_i is the body force per unit mass, ρ is the mass per unit volume of the medium, and $\frac{\partial \upsilon_i}{\partial t}$ is the material derivative of the velocity. Initially, new strain rates are computed from the known nodal velocities for each zone. All the constitutive models have a similar numerical algorithm, which can be represented by a general equation, as shown in Eq. (2). These equations are invoked to calculate the new stresses using the incremental form H^*_{ij} from the strain rate and the stresses from the previous time.

$$\overset{\vee}{\sigma}_{ij} = H^*_{ij}(\sigma_{ij}, \Delta\varepsilon_{ij}, k) \tag{2}$$

where, $\overset{\vee}{\sigma}_{ij}$ is the co-rotational stress rate tensor, σ_{ij} is the stress rate tensor, H^*_{ij} is the constitutive function, $\Delta\varepsilon_{ij}$ is the strain rate tensor, and k is a parameter which takes into account the loading history. The strain rate tensors are computed from the known velocity field component for each zone using the finite-difference formulation as given in Eq. (3),

$$\Delta\varepsilon_{ij} = -\frac{\Delta t}{6V}\sum_{l=1}^{4}(\upsilon_i^l n_j^l + \upsilon_j^l n_i^l)S^l \tag{3}$$

where, V is the volume of the zone, v^l_i is the translational velocity at a material node, n^l_j over a time interval Δt. For a large strain method, the stress tensors are corrected for rotational strain as shown below,

$$\Delta\sigma_{ij} = \Delta\overset{\vee}{\sigma}_{ij} + \Delta\sigma^C_{ij} \tag{4}$$

where, $\Delta\sigma^C_{ij}$ is stress correction. Finally, for each time step, from the previous velocity and forces, the equation of motion is used to define the new nodal velocities and displacements from which the new strain rates and stress are calculated. These new stress and strain obtained are used to update the force vector.

For fluid soil coupling, the pore pressure developed can be evaluated to calculate the effective stress of the solid. In the present study, the variables involved in the description of the fluid flow through porous media are pore pressure, saturation, and specific discharge. These variables can be related through the fluid mass balance equation, Darcy's law for fluid transport, which can specify the fluid response to change in pore pressure, saturation, and volumetric strain. The substitution of this fluid mass equation into fluid constitutive relations gives a differential equation in terms of pore pressure and saturation as in Eq. (5).

$$\frac{1}{M}\frac{\partial p}{\partial t} + \frac{n}{\rho}\frac{\partial S}{\partial t} = \frac{1}{S}(-q_{i,i} + q_v) - \alpha\frac{\partial \varepsilon}{\partial t} \tag{5}$$

where, M is the Biot modulus (in N/m^2), q_v is the volumetric fluid source intensity (in 1/s), n is the porosity, and α is the Biot coefficient. The changes in the variation of the fluid content are measured in terms of pore pressure (p), saturation (S), and mechanical volumetric strain (ε). This may be solved for a particular geometry, property, boundary, and initial conditions. The final solution is reached when the body is in equilibrium, and the out of balance force becomes a very small value.

In the present study, a 40 m long, 1 m wide, and 24 m deep continuum soil medium is considered. The main criteria deciding the time and accuracy in the finite-difference analysis is choosing the most appropriate type and size of mesh (Gregor and Shobayry 2011). Radially graded mesh called "radcylinder" is selected for the zones around the cylindrical underground structure. The remaining areas are meshed using brick elements. For zoning, Lysmer and Kuhlemeyer (1969) proposed that the maximum size of the spatial element, Δl, must not be greater than one-tenth or one-eighth of the wavelength of the input motion with the most significant frequency. The

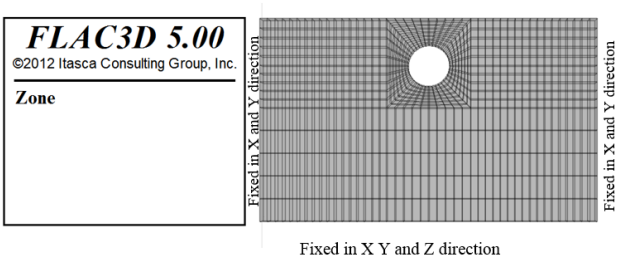

Fig. 3 Finite difference model used

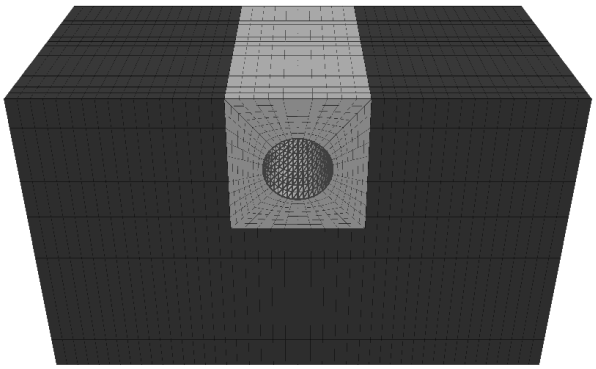

Fig. 4 Three-dimensional finite-difference model with the replacement method

accurate transmission of the wave is ensured by discretising the entire domain with and without the replacement into 840 zones, taking this criterion into consideration. The finite-difference model used for the underground structure buried in the in-situ sand is represented in Fig. 3.

3D FD modelling of the underground structure embedded on a 40 m long, 10 m wide, and 24 m deep continuum soil medium is also performed to study the various factors of replacement method influencing the liquefaction-induced uplift of the structure. The underground structure is embedded at a shallow depth of 5.5 m from deep homogenous Houston sand with a relative density of 52%. The entire 3*D* model is discretised into 15200 zones using brick elements of size 0.5 m in X, Y, and Z directions near the base of the model and radially cylindrical elements near the structure. The 3*D* FD model used to study the factors affecting the uplift of the underground structure with replacement method is shown in Fig. 4.

Another essential criterion to be considered in the numerical study is the boundary conditions. Before considering the dynamic response of the structure, the entire model has to be brought to its initial static equilibrium by considering only the geometrical dead weight of the soil. Hence, the whole model is fixed in X, Y, and Z directions at the base, and the top is kept free. The lateral boundaries are restrained in X and Y directions. To study the dynamic response of the soil, the vertical boundaries are assumed to be placed at a sufficient distance to minimise the reflection of the outward propagation wave and to achieve a free field condition (Chian *et al*. 2014). Additionally, the base is considered as an impermeable boundary, whereas the ground surface is considered as a free drainage boundary.

3.1 Material models

The behaviour of the sand in the present numerical study is defined using an elastic-perfectly plastic Mohr-Coulomb model. The development of pore pressure due to the ground shaking is estimated using the Finn-Byrne formulation, which is used along with the Mohr-Coulomb plasticity model (Finn 1981, Byrne 1991, Azadi and Hosseini 2010a, Sudevan *et al*. 2018, Sudevan *et al*. 2020). The pore pressure developed is estimated by knowing the volumetric strain increment, $\Delta\varepsilon_{vd}$, which is related to the cyclic shear strain amplitude, γ by a two-parameter equation, as shown in Eq. (6) (Byrne 1991). From the normalised standard penetration number $(N_1)_{60}$ of the sand, the two parameters for the estimation of the volumetric strain increment are obtained using Eqs. (7) and (8).

$$\frac{\Delta\varepsilon_{vd}}{\gamma} = C_1 \exp(-C_2 \frac{\varepsilon_{vd}}{\gamma}) \tag{6}$$

$$C_2 = \frac{0.4}{C_1} \tag{7}$$

$$C_1 = 8.7(N_1)_{60}^{-1.25} \tag{8}$$

$$D_r = 15(N_1)_{60}^{1/2} \tag{9}$$

where, D_r is the relative density of the sand, and C_1 and C_2 are parameters that control the volume change and shape of the accumulated volume change with the number of cycles. Using Eq. (10) the pore pressure accumulated is estimated from the known volumetric strain increment (Byrne 1991):

$$\Delta u = E_r \Delta\varepsilon_v \tag{10}$$

where, Δu is the incremental pore water pressure, and E_r is the rebound modulus of the sand skeleton. The in-situ soil considered in the present study is cohesionless sand, and the properties of the fine sand and the coarse sand used is the same as that used by Chian and Madabhushi (2013) in their study (see Table 1). The elastic modulus of the fine sand based on the SPT was calculated from the correlation postulated by Kulhawy and Mayne (1990), as shown in Eq. (11) and the elastic modulus for coarse sand is computed using the empirical relation as in Eq. (12) (Bowels 1996). The bulk modulus and shear modulus of the sand used in the numerical analysis is estimated using Eqs. 13(a) and 13(b), respectively, and are shown in Table 1. The permeability of the coarse sand was considered as 200 times more than that of the fine sand to bring in the effect of enhanced drainage of excess pore water accumulated near the structure (Seed and Booker 1976).

$$\frac{E_s}{P_a} = 10(N_1)_{60} \tag{11}$$

$$E_s = 1200(N+6) \tag{12}$$

$$K = \frac{E}{3(1-2\mu)} \tag{13a}$$

Table 1 Soil properties used

Parameters	Houston Sand			Fraction B Sand
Relative density	45	52	65	45
Dry density (kg/m^3)	1450	1490	1520	1580
Initial void ratio	0.8	0.77	0.71	0.67
Internal friction angle (^{0})	33	33	33	33
Bulk modulus (MPa)	10.20	14.28	16.32	18.36
Shear modulus (MPa)	3.74	5.24	5.98	6.73
Permeability (m/s)	10^{-3}	10^{-3}	10^{-4}	10^{-1}

$$G = \frac{E}{2(1+\mu)} \tag{13b}$$

where, E_s is the elastic modulus, P_a is the atmospheric pressure and $(N_1)_{60}$ is the SPT value corrected for the field procedure to an average energy ratio of 60%, K and G are the bulk modulus and shear modulus of the sand respectively, μ is the poissons ratio.

The concrete underground structure (μ= 0.33) used in the present study is defined using 80 shell-type elements. The interface between the soil and the underground structures has a small friction angle (φ) of 21.8^0. The Mohr-Coulomb strength failure criterion is used to characterise the strength of the interface used. The interface stiffness values k_n and k_s in the normal and tangential directions affect the relative movement of the structure and is calculated using Eq. (14) (Itasca consulting group 2012).

$$k_n = k_s = 10 \times \left[\frac{K + \frac{4}{3}G}{\Delta z_{\min}} \right]_{60} \tag{14}$$

where, K and G are the bulk and the shear modulus respectively, and $[\Delta z]_{min}$ is the smallest dimension of the contact zone adjacent to the interface in the normal direction.

3.2 Type of analysis

Initially, static equilibrium analysis is carried out until the whole model reaches a state of static equilibrium. Once the entire model has attained the state of equilibrium, subsequent changes in the loading condition are made in order to carry out the dynamic analysis. Dynamic analysis is based on the explicit finite difference formulation, which can be coupled to structural elements and the groundwater flow, thus enabling to conduct a fully coupled soil-structure problems due to ground shaking. The base of the model was considered to be rigid. To study the uplift response an acceleration time history was applied at the base of the model as boundary motion. A sinusoidal input motion with peak input acceleration of 0.1 g and frequency of 0.75 Hz for a total duration of 28 s, which is same as that used by Chian and Madabhushi (2013) in their experimental studies, was adopted in the present study. The tetrahedron subzone volume, p-wave velocity, and the stiffness-proportional damping mainly decide the time step for the dynamic analysis. The dynamic analysis was carried out for the following cases:

i) The pore pressure and the uplift response of the underground structures without replacement of the in-situ soil

ii) The pore pressure and the uplift response of the underground structures where surrounding soils are replaced with coarse materials. In this case, the effect of various factors, such as the width of replacement, and different schemes of replacement for mitigating the uplift response of the underground structure, are analysed. Apart from this, the continuous replacement of in-situ sand and replacement with regular intervals between the replaced area are compared.

4. Response of the underground structure without replacement of the natural soil

The liquefaction-induced uplift of the underground structure buried in homogeneous in-situ sand (without replacement of natural soil) for various relative density and depth is carried out. The results are presented in terms of the pore pressure response near the underground structure and the resulting uplift of the structure. The results obtained from the FD analysis are compared with the results obtained by Chian and Madabhushi (2013) from their experimental studies. In addition, the far-field pore pressure response and the acceleration response developed within are studied.

4.1 Validation of the FD model

The pore pressure response observed at the invert and the crown of the underground structure buried at a depth of 5.5 m from the ground surface (without replacement of soil) is shown in Fig. 5. When the relative density is 45%, around 50 kPa of pore pressure is observed at the invert of the structure, whereas when the relative density is 65%, a maximum of about 25 kPa is observed at the invert of the structure. With an increase in the density, the pore pressure accumulated at the invert reduces by around 50%. The excess pore water pressure generated at the invert and the crown of the structure are compared with results observed by Chian and Madabhushi (2013) in their experimental study. It is noted that when the relative density of the soil is 52%, the excess pore pressure obtained from the present study at the invert of the structure is overestimated for the initial 10 *s*. Thereafter, the model gives an excess pore pressure of about 30 *kPa*. At the crown, when the relative density of soil is 52%, both the results from the present study and the experimental study by Chian and Madabhushi (2013) showed a good match. However, when the relative density of the soil is 65%, pore pressure responses obtained by Chian and Madabhushi (2013) from their experimental study at the invert and the crown passes through the lower bound points of those obtained from the present study. Overall, the excess pore pressure obtained at the invert and the crown of the structure is comparable with that obtained

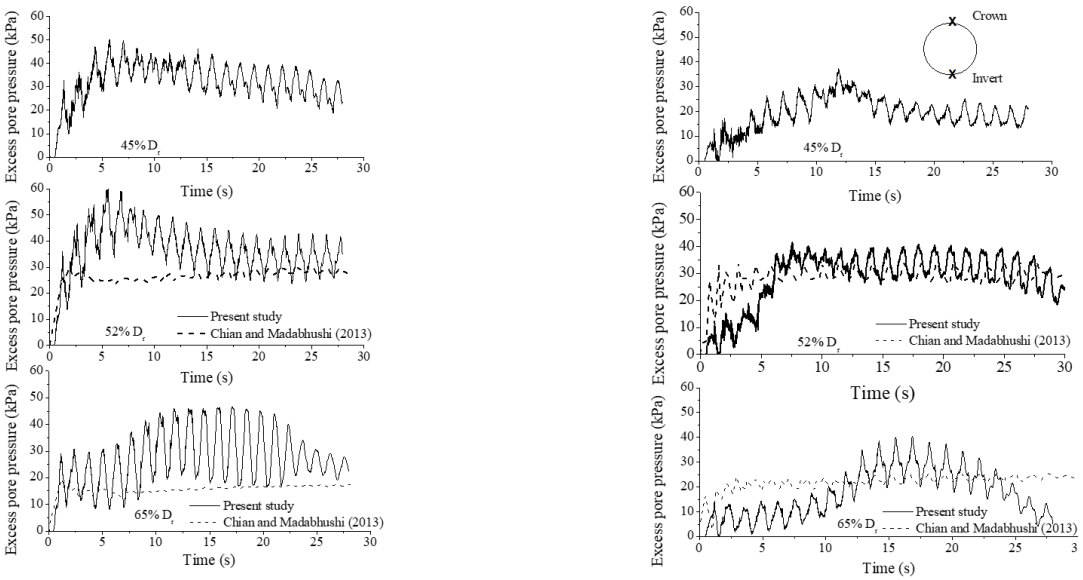

(a) At invert (b) At crown

Fig. 5 Comparison of excess water pore pressure developed at the invert and crown of the structure without replacement

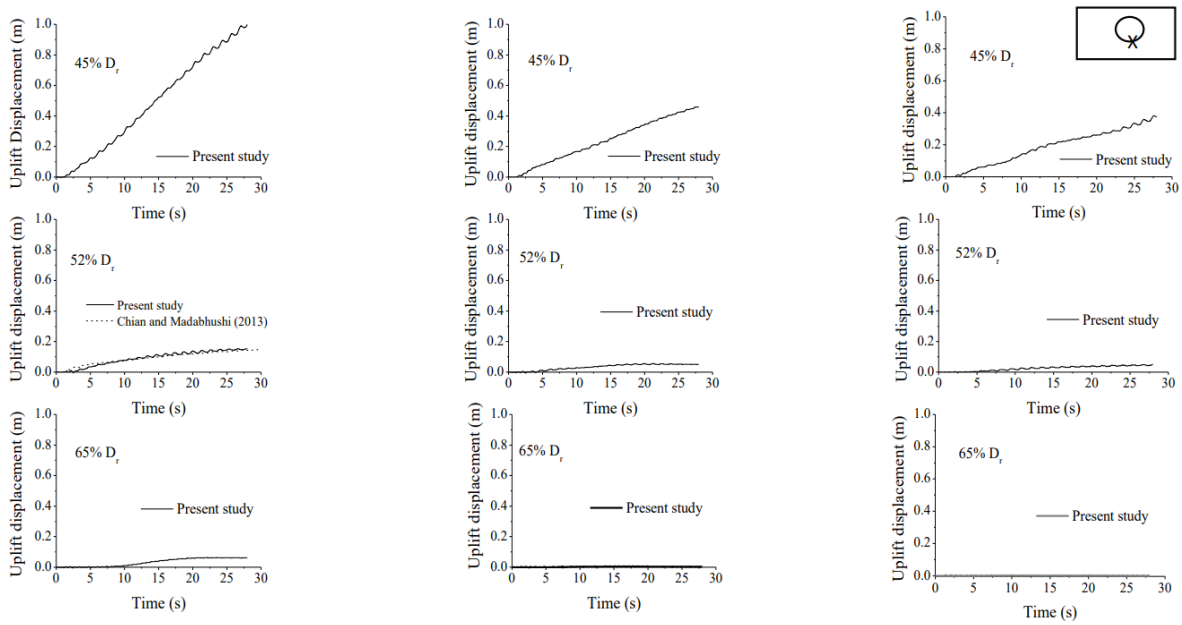

(a) h=1.1D (b) h=1.3D (c) h=1.5D

Fig. 6 Effect of depth of embedment on the uplift of the structure (without replacement)

by Chian and Madabhushi (2013). In Fig. 5, it is visible that the pore pressure accumulated at the invert of the structure reduced after 15 *s* for all the cases. During the uplift, a void space will be formed below the structure, which eventually reduces the pore pressure at the invert of the structure.

The variation in the liquefaction-induced uplift of the underground structure buried into the in-situ fine sand (without replacement) at embedment depths of 1.1*D*, 1.3*D*, and 1.5*D* are shown in Fig. 6(a)-6(c) respectively. In all the cases, the structure started to show gradual lifting after a minimum time of 3 s, i.e., when the uplifting force overcomes the resisting force. It is observed that in all the cases, the structure gets uplifted after few seconds and thereafter increases continuously till the shaking ceases. From Fig. 6, it is observed that with increasing density of the in-situ soil (i.e., when D_r increases from 45% to 65%), the uplift reduces considerably. When the soil density is 65%, the uplift is negligible in all cases. It is because when the soil is dense, the pore pressure accumulated at the invert of the structure is very low. This led to a low uplifting force on the structure to displace it. From the present, the uplift observed by the underground structure embedded at a depth of 1.1*D* within saturated sand of relative density 52% is about 0.15 m, and it is matching well with that observed by Chian and Madabhushi (2013) in their experimental study. As shown in Fig. 6(a), for the case when the structure is embedded at a depth of 1.1*D*, the uplift of the underground structure is 0.9 m in the sand with 45% relative density.

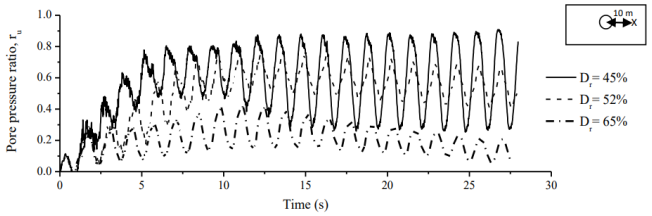

Fig. 7 Pore pressure response at far-field at 8 m depth (without replacement of soil)

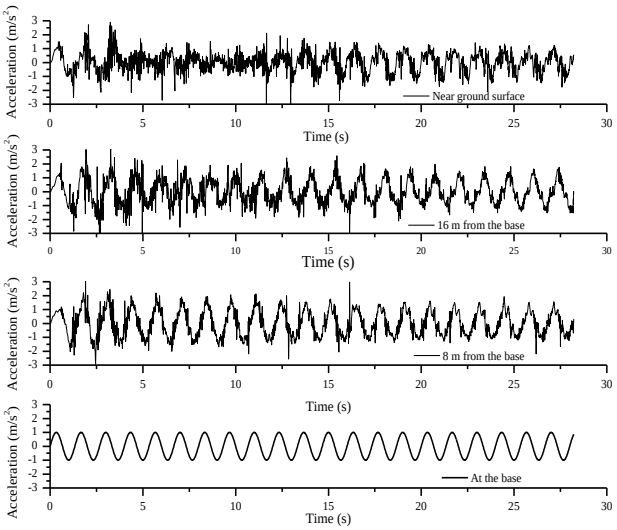

Fig. 8 The far-field acceleration time history

Whereas, when the soil density is 65%, the uplift observed is as low as 0.061 m indicating a 95% reduction in the uplift with increasing density of the in-situ sand. A similar reduction in the uplift is observed by increasing the depth of embedment to 1.3*D* and 1.5*D* and is shown in Fig. 6(b) and 6(c).

4.2 Far-field pore pressure response

The pore pressure response developed away from the underground structure at a depth of 8.0 m (without any replacement) at various relative density is shown in Fig. 7. The pore pressure ratio, r_u, is the excess pore water pressure normalised to the initial effective stress of the sand, and it is used to study the pore pressure response. The pattern of the pore pressure generated is similar for all the relative densities considered in the present study. In all the cases, as shown in Fig. 5, the pore pressure increases rapidly with time up to a maximum value. After reaching the maximum value, pore pressure remains constant for the rest of the duration of the shaking. It is worth noting that the negative spikes are observed in the pore pressure response, which is caused due to the dilative response within liquefiable soil. Similar results have been observed by Dobry *et al*. (1988), Fiegel and Kutter (1994), and Elgamal *et al*. (1998) in their study. Theoretically, liquefaction is triggered in the soil when the excess pore pressure within the sample approaches the initial effective stress of the soil, i.e., when the pore pressure ratio reaches one. However, in the present study, the soil liquefaction is triggered, in large strain condition when the r_u value is about 0.7, as assumed by Kammerer *et al*. (2004), Wu *et al*. (2004) and Chian *et al*. (2014). Further, when the soil is relatively loose, i.e., when D_r= 45%, the pore pressure ratio reaches a maximum of about 0.8. With the increase in density of the in-situ soil, the maximum pore pressure ratio obtained reduces considerably. Moreover, when the relative density of the soil is about 65%, the maximum pore pressure ratio became as low as 0.2, which indicated that the soil did not liquefy. Ling *et al*. (2003) and Madabhushi and Madabhushi (2015) observed similar behaviour of pore pressure increase and dilation spikes in their experimental studies.

4.3 Far-field acceleration time response

The comparison of the far-field acceleration response for 28 s of shaking at the base and at depths of 16 m, 8 m, and 1 m in the soil of 45% relative density is shown in Fig. 8. It is observed that as the shear wave propagates upwards, for the first few cycles, the acceleration response was strong, and later it attenuated as the soil liquefied. It is observed that the acceleration remains more or less the same throughout the entire depth. After the soil attained maximum pore pressure, the acceleration did not attenuate to a smaller value. From the figure, it is visible that when the shear wave reached near the surface, the maximum acceleration magnitude is less than 0.1 g, and therefore, the shear wave got dampened. Pore pressure was generated within the soil model due to shaking and this reduced the stiffness of the soil, which affected the effective propagation of the shear wave (Lombardi and Bhattacharya 2016).

From literature (Koseki *et al*. 1997b, Orense *et al*. 2003, Tobita *et al*. 2011), it is clear that the uplift of the structure occurs when the uplifting force acting on it overcomes the resisting force acting against the uplift. The uplifting force acting on the structure comprises of the upward force from the excess pore water pressure developed during an earthquake (U_{ru}) and the uplift force due to the hydrostatic pressure (U_h). The resisting force comprises of the weight of the structure (W_s), the weight of the overburden acting above the structure (W_b), and the frictional resistance acting against the structure and the surrounding soil (Q_s), as shown in Fig. 9. Therefore, the factor of safety (F_s) against the uplift of the underground structure due to liquefaction of the soil can be considered as a ratio between the resisting force and the uplift force acting on the structure (Koseki *et al*. 1997b, Orense *et al*. 2003, Tobita *et al*. 2011) and is given in Eq. (15):

$$F_s = \frac{W_s + W_b + Q_s}{U_{ru} + U_h} \tag{15}$$

where,

$$W_s = \frac{\Pi}{4}(D_0 - D)\gamma_{structure} \tag{16}$$

$$W_b = \left[(D*h) + \left(\frac{D^2}{2} - \frac{\pi}{8}D^2\right)\right]\gamma_{sat} \tag{17}$$

$$U_h = (D^*(D+h))\Upsilon_w \quad (18)$$

where, D_o is the outside diameter of the underground structure, D is the inner diameter of the underground structure, h is the distance between the ground surface till the springing of the structure, Υ_w is the unit weight of water, and $\Upsilon_{structure}$ is the structures unit weight. When the soil liquefies, the frictional resistance acting between the structure and the soil (Q_s) is negligible and therefore, it is considered to be zero (Orense *et al*. 2003). As per Eqs. (16) and (17), the resisting force due to the weight of the structure (W_s) is 19.63 kN, and to the sand above the structure (W_b) is 0.379 kN. The uplift force (U_h) due to the hydrostatic pressure at a depth of 8 m from the ground surface, as per Eq. (18), is 0.078 kN. The upward force (U_{ru}) exerted by the accumulated pore pressure at the invert of the structure will be 19.93 kN, to attain a minimum factor of safety of 1. This indicates that a threshold pore pressure ratio of about 0.2 developed below this structure initiates the uplift of the structure. In this case, the pore pressure ratio below the structure need not reach 1.0 for uplift to happen. Threshold pore pressure is the minimum pore pressure ratio that needs to be developed at the invert of the structure considered so that the upward force acting at the invert is just sufficient to cause the structure to displace from its position. Therefore, it can be observed that for the structure to be uplifted, the soil around the structure need not liquefy, if the structure is very light and the vertical equilibrium of the forces is not respected when the excess pore pressure increases. The uplift of the underground structure increases further with more accumulation of the pore water at the invert of the structure, i.e. when the pore pressure ratio becomes greater than 0.2. When the relative density of the soil is 65%, a very small pore pressure ratio of about 0.35 is exerted at the invert of the structure. Since the critical pore pressure ratio is 0.2, a very small negligible uplift is observed. Whereas, when the sand has densities of 52% and 45% higher pore pressure ratios of 0.75 and 0.9 are attained at the invert of the structure, leading to higher uplifts of 0.2 m and 1.0 m, respectively.

5. Estimation of the liquefaction-induced uplift of the underground structure

From the present study, the uplift of the underground structure as a result of liquefaction of the soil can be generalised using Eq. (19).

$$\frac{U}{D} = 0.5 - 0.005D_r - 0.131\frac{h}{d} \quad (19)$$

where, U is the maximum uplift of the structure (in m), D is the diameter of the structure (in m), D_r is the relative density of the soil (in %), and h is the embedment depth of the structure (in m). The constant related to the h/D is quite significant, which indicates that maximum uplift observed varies with the depth of embedment of the structure. Even though the relative density of the soil plays a vital role in the displacement of the structure, the depth of embedment of the structure is more significant.

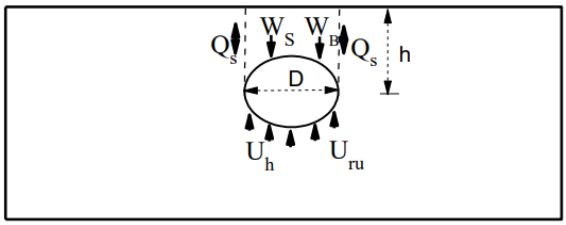

Fig. 9 Forces acting on the structure during liquefaction of the soil

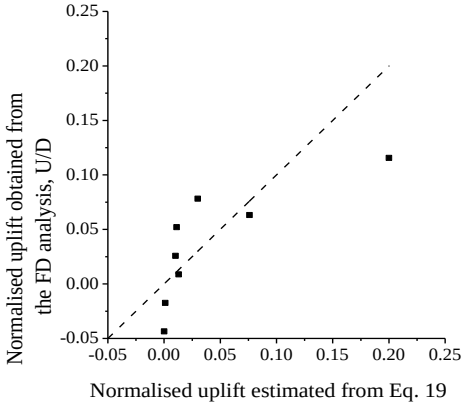

Fig. 10 Comparison of normalised uplift of the structure (without replacement) as computed from the FD analysis and that estimated from Eq. (19)

The normalised uplifts obtained from the FD analysis and the Eq. (19) are compared in Fig.10. It is seen that only a small deviation in the values are obtained from the mean line. Thus, a good agreement is obtained between the normalised uplift from the FD analysis and that obtained from Eq. 19. It can be seen that a good fit to the data is achieved with an R^2 value of 0.60. A chi-square test was conducted to claim the goodness of fit of the predictive equation. As per the hypothesis, H_o is the null hypothesis in which the predicted equation fits the data, and H_1 is the alternative hypothesis where the predicted equation does not fit the data. Considering a 95% confidence level, $\chi^2_{0.05,7}$ is 14.067. The computed χ^2_0 is 0.074, which is less than the $\chi^2_{0.05,7}$; thereby, it is unable to reject the null hypothesis, H_o and that the Eq. (19) predicts the uplift of the structure with a good fit. For the case when the density of the soil is 65%, the FD analysis indicated a settlement, whereas a zero displacement was predicted using the Eq. (19).

6. Response of underground structure with the continuous replacement of in-situ soil

In the following section, the performance of continuous replacement of in-situ sand with coarse sand on the uplift of the underground structure is studied. Two schemes of replacement are studied: replacement of in-situ sand above the springing (replacement method 1) and that around the structure (replacement method 2), as shown in Fig. 2. In this case, the pore pressure and the resulting uplift of the underground structure, which is buried at a depth of 7.5 m from the ground surface in the sand with a relative density

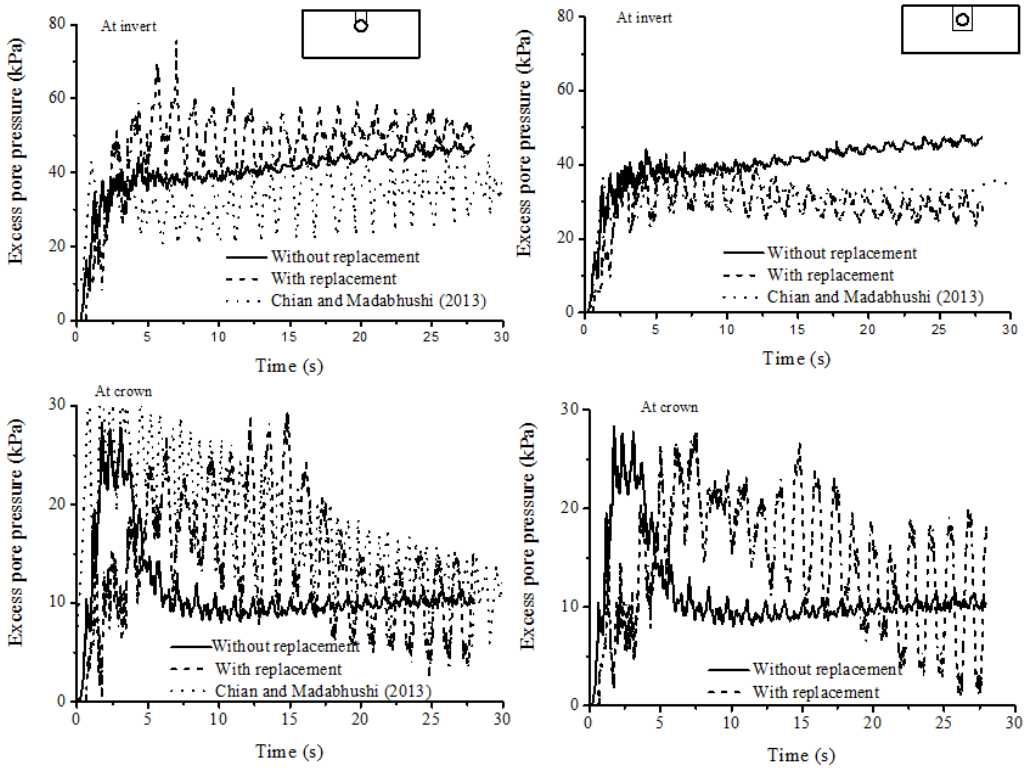

(a) Replacement method 1 (b) Replacement method 2

Fig. 11 Excess pore water pressure developed around the structure using (a) replacement method 1 and (b) replacement method 2 (h= 7.5 m, D_r= 45%)

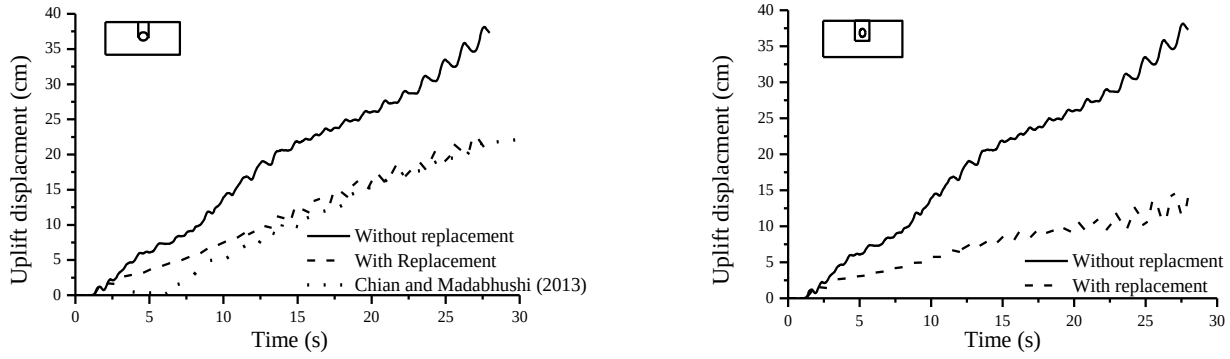

(a) Replacement method 1 (b) Replacement method 2

Fig. 12 Uplift response of the underground structure using (a) replacement method 1 and (b) replacement method 2 (h= 7.5 m, D_r= 45%)

of 45%, are studied. The pore pressure and uplift response obtained from the numerical analysis are validated with the centrifuge studies reported by Chian and Madabhushi (2013).

6.1 Pore pressure response

The excess pore water pressures developed at the invert and the crown of the structure for replacement method 1 and replacement method 2 are shown in Fig. 11. It is observed that, when replacement method 1 is used, the pore pressure observed at the invert is about 40 kPa, which is the same as that observed without any replacement. Whereas, when replacement method 2 is used, a considerable reduction in the pore pressure accumulation is observed at the invert of the structure. However, for both the methods, the pore pressure generated around the structure reduced considerably, due to the more permeable soil near the structure which resulted in accelerated dissipation of the pore water accumulated (Wang *et al*. 2012). In replacement method 1, the pore water accumulated around the structure, especially at the invert of the structure, is almost double compared to that observed with the replacement method 2. A reduced pore water accumulation of about 30 kPa is observed at the invert, when replacement method 2 is used. This results in a reduced upward force acting at the invert of the structure. Whereas for the replacement method 1, due to a higher pore pressure accumulation at the invert, a higher

magnitude upward force is experienced at the invert. The higher pore pressure observed in the case of replacement method 1, which makes the structure more buoyant as compared to that in the replacement method 2. The present study results using the replacement methods are compared with the results obtained by Chian and Madabhushi (2013) in their centrifuge study. The results are matching well with the pore pressure response observed near the structure. However, the excess pore water pressure observed at the invert of the structure using the replacement method 1 is overestimated compared to the results obtained by Chian and Madabhushi (2013).

6.2 Uplift response

The plot comparing the uplift of the underground structure with and without replacement methods is shown in Fig. 12. In both cases, the general trend of the uplift response of the underground structure are similar. From the figure, it is observed that an uplift of about 0.37 m is observed when there is no replacement of sand near the structure. In the case, when replacement method 1 is used, a maximum uplift of about 0.22 m is observed. Whereas, when replacement method 2 is employed, a reduced uplift of about 0.13 m is observed. This reduction in the uplift with replacement method 2 is due to the reduced pore pressure accumulated at the invert of the structure. Using replacement method 2, about 62% reduction is observed compared to the case without replacement, whereas a 38% reduction in the uplift is observed when replacement 1 is used. However, a small uplift is observed in replacement method 2, which is due to insufficient resistance against the uplift due to the shallow burial depth of the underground structure.

The uplift obtained using the replacement method 1 from the present study is compared with the experimental results by Chian and Madabhushi (2013), as shown in Fig. 12(a) and it is found to be matching quite well.

7. Factors influencing uplift of the underground structure with continuous replacement

In the following section, the continuous replacement of in-situ sand near the structure for varying width and different schemes are studied. In this case, the pore pressure and the resulting uplift of the underground structure, buried at a depth of 5.5 m from the ground surface in sand with a relative density of 52%, are studied.

7.1 Width of replacement

To study the effect of the width of replacement to reduce the liquefaction-induced uplift of the structure, we considered three cases: i) replacement with width D, ii) replacement with width $2D$, and iii) replacement with width $3D$. They are shown in Fig. 13. For the case without replacement, a maximum pore pressure ratio of about 0.6 is observed at the invert of the structure due to shaking. By replacing the in-situ soil near the structure, the pore pressure accumulated near the structure is reduced. For the

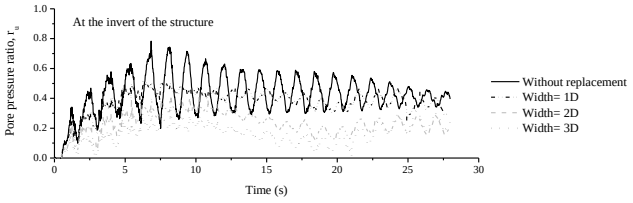

Fig. 13 Effect of the width of replacement on pore pressure response (h= 5.5 m, D_r= 52%)

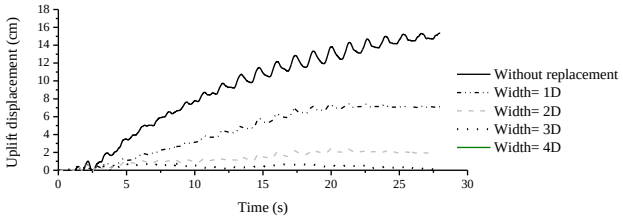

Fig. 14 Effect of the width of replacement on the uplift of the underground structure (h= 5.5 m, D_r= 52%)

cases when the width of replacements are $2D$ and $3D$, the maximum pore pressure ratio at the invert is not more than 0.2. Whereas, when the width of replacement is D, a maximum pore pressure ratio of about 0.5 is observed at the invert of the structure.

The liquefaction-induced uplift of the underground structure, due to the replacement of in-situ fine sand with coarser sand, is shown in Fig. 14. For the case, without replacement of the in-situ sand, a maximum uplift of about 0.15 m is observed. It is seen that when D width of fine sand is replaced, due to higher accumulation of the pore water around the structure, a higher uplift is observed compared to when $2D$ and $3D$ widths are replaced. The reductions in uplift when $2D$ and $3D$ widths are replaced are almost negligible and are as small as 10 mm. In addition to the accelerated drainage of the pore water near the structure, higher overburden force acting on the structure increases the resisting force acting against the liquefaction-induced uplift. However, considering the economy and safety, minimum width of $2D$ replacement is suggested for an effective reduction in the uplift of the underground structure.

7.2 Schemes of replacement

In the present study, three schemes of replacement are considered: replacement of fine sand above the structure till the springing (replacement method 1), replacement of fine sand around the structure (replacement method 2), and replacement of sand below the springing level of the structure (replacement method 3). These three schemes of replacement methods are carried out by replacing in-situ sand of width $2D$ with coarse sand and are compared with the case without replacement.

The pore pressures generated around the underground structure along with the three schemes of replacement are studied in terms of the excess pore water pressure generated at the invert of the structure (see Fig. 15). From the figure, it is observed that a maximum pore pressure ratio of about 0.6 is observed when no replacement was considered,

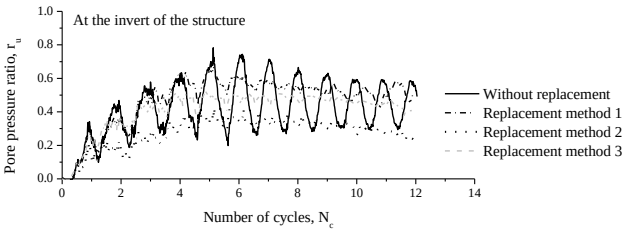

Fig. 15 Effect of different scheme of replacement method on the pore pressure response (h= 5.5 m, D_r=52%)

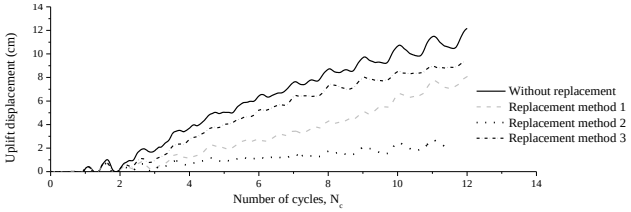

Fig. 16 Effect of different scheme of replacement method on uplift of the structure (h= 5.5 m, D_r= 52%)

whereas a pore pressure ratio of about 0.5 is observed for replacement methods 1 and 3. The maximum pore pressure ratio as low as 0.2 is observed when replacement method 2 is used. In the case of replacement method 1, as the replaced area is confined to the region above the springing, a higher pore water accumulation is observed at the invert of the structure. Whereas, when replacement method 2 is used, the pore water accumulated at the invert of the structure is very low resulting in a small uplift force compared to the case without replacement and case where replacement method 1 and 3 is used. These drain materials form a non-liquefiable zone of soil around the structure, thereby reducing the pore pressure accumulation around the structure. Similar observations were made by Rasouli *et al.* (2018) in their experimental studies.

The uplifts of the underground structure with varying number of cycles using three scheme of replacement are shown in Fig. 16. From Fig. 15, it is observed that for the case without replacement and those using replacement methods 1 and 3, the pore pressure accumulated was maximum at about one cycle of loading whereas, for replacement method 2, maximum pore pressure is accumulated at about two cycles. Therefore, from Fig. 16, it is observed that the uplift occurs after one cycle in case of replacement methods 1 and 3, whereas uplift occurs after two cycles in case of replacement method 2. In all the cases, the structure showed uplift as long as the shaking exists. It is observed that a maximum uplift of about 0.10 m uplift is observed for the case for no replacement is used, whereas 0.08 m and 0.09 m are attained when replacement methods 1 and 3 are used. Reduced uplift of about 0.02 m is observed when replacement method 2 is used. Due to the replacement of the soil around the structure using coarse sand, there is a reduction in uplift by 80% as compared to the case without replacement and a reduction about 50% reduction compared to the replacement methods 1 and 3. Presence of coarse sand around the structure accelerates the drainage of the pore water accumulated from the vicinity of the structure. As a result, the uplifting force acting on the

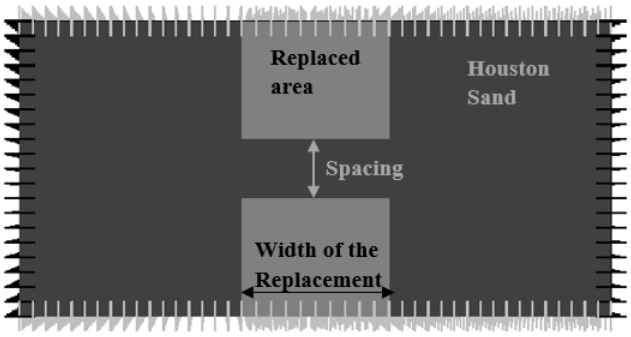

Fig. 17 Schematic view of the replacement method with a regular interval (plan view)

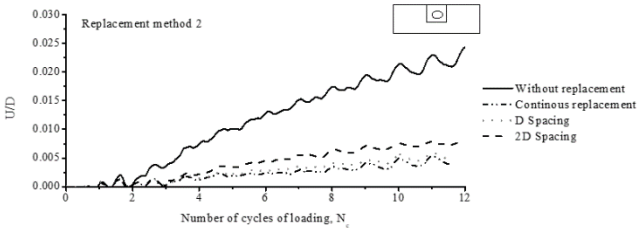

Fig. 18 Normalised uplift of the structure versus the number of cycles of loading for different replacement methods (h= 5.5 m, D_r= 52%)

structure reduces and uplift occurs. Whereas, when the soil above the structure is replaced as in replacement method 1, a high pore pressure accumulation is observed at the invert of the structure. Hence, a larger uplift force will be acting at the invert and results in a higher uplift. However, maximum uplift is observed using replacement method 3 as there is no drainage path for the accelerated dissipation of the pore water accumulated at the invert.

8. Continuous replacement versus replacement with regular interval

The liquefaction-induced uplift of the underground structure obtained from the case with continuous replacement is compared with that computed for the replacement with regular interval. For this, four cases are considered: (i) no replacement, (ii) continuous replacement, (iii) replacement with *D* width spacing, and (iv) replacement with 2*D* width spacing, as shown in Fig. 2. The in-situ sand of width 2*D* is replaced continuously and with regular intervals. The plan of the model understudy with a regular interval is shown in Fig. 17.

The uplift of the structure normalised to the diameter of the structure (*U/D*) and its variation with the number of cycles of loading is shown in Fig. 18. The case with continuous replacement led to a small uplift of about 0.005*D*. When the spacing between the replaced regions is 2*D* width, a reduction of about 50% in the uplift is observed as compared to that of the case without any replacement. As the spacing between the replaced zones is reduced, the slope of the trend line becomes steeper, implying more effective mitigation as large as 80% as compared to that of the case without any replacement. The reduction in the liquefaction-

induced uplift for continuous replacement and replacement with D interval is almost the same. However, it is not economical to replace the fine sand for the entire length. Hence considering safety and economical aspects, a spacing of around D width can be employed to reduce the uplift of the underground structures due to liquefaction of the soil. Moreover, the volume of the replacement material required for the replacement with regular interval can be reduced by 50% compared to the continuous replacement method.

9. Conclusions

In this paper, numerical modelling of liquefaction-induced uplift of an underground structure with and without replacement of in-situ fine sand around the structure with coarse sand by different methods was carried out using FD code, FLAC3D. The numerical results were validated with the centrifuge results reported by Chian and Madabhushi (2013). Based on the above study, the following major conclusions are arrived:

• As can be seen from the study without replacement, the in-situ sand with an initial relative density of 65% would not liquefy and thus, results in negligible liquefaction-induced uplift. Hence the liquefaction-induced uplift can be prevented by densification of the in-situ sand with relative density above 65%.

• An empirical equation for the maximum liquefaction-induced uplift of the underground structure is proposed, and it mainly depends on the depth of embedment and the relative density of the soil.

• The replacement of in-situ liquefiable fine sand using coarse sand was carried out using three methods: replacement above the springing level of the structure, around the structure, and below the spring level of the structure. Among these methods, replacement method no 2, where fine sand is replaced around the structure, was found to be most effective for the reduction of the liquefaction-induced uplift of the underground structure. It is due to the accelerated drainage of the pore water occurs around the underground structure.

• For the case of continuous replacement, it is found that a maximum reduction of 50% of liquefaction-induced uplift can be achieved by the replacement of fine sand with a width 2D with coarse sand.

• The performance for the case of replacement with an interval of D spacing and 2D width is found to be comparable with that obtained for continuous replacement of similar width.

• Despite the difficulties in the implementation of replacement with a regular interval, one of the major advantages of this replacement method is that the volume of the replacement material can be reduced by about 50%.

References

Adalier, K., Abdoun, T., Dobry, R., Phillips, R., Yang, D. and Naesgaard, E. (2003), "Centrifuge modelling for seismic retrofit design of an immersed tube tunnel", *Int. J. Phys. Model. Geotech.*, **3**(2), 23-35. https://doi.org/10.1680/ijpmg.2003.030203.

Arango, I. (2008), "Earthquake engineering for tunnels and underground structures, a case history", *Geotech. Earthq. Eng. Soil Dyn.*, **181**, 1-34. http://doi.org/10.1061/40975(318)205.

Aydingun, O. and Adalier, K. (2003), "Numerical analysis of seismically induced liquefaction in earth embankment foundations. Part I. Benchmark model", *Can. Geotech. J.*, **40**(4), 753-765. https://doi.org/10.1139/t03-025.

Azadi, M. and Hosseini, S.M.M.M. (2010a), "The uplifting behavior of shallow tunnels within the liquefiable soils under cyclic loadings", *Tunn. Undergr. Sp. Tech.*, **25**(2), 158-167. https://doi.org/10.1016/j.tust.2009.10.004.

Azadi, M. and Hosseini, S.M.M.M. (2010b), "Analyses of the effect of seismic behavior of shallow tunnels in liquefiable grounds", *Tunn. Undergr. Sp. Tech.*, **25**(5), 543-552. https://doi.org/10.1016/j.tust.2010.03.003.

Bao, X., Xia, Z., Ye, G., Fu, Y. and Su, D. (2017), "Numerical analysis on the seismic behavior of a large metro subway tunnel in liquefiable ground", *Tunn. Undergr. Sp. Tech.*, **66**, 91-106. https://doi.org/10.1016/j.tust.2017.04.005.

Bowels, A.J. (1996), *Foundation Analysis and Design*, 5th Edition, McGraw International Editions, Singapore.

Brennan, A.J. and Madabhushi, S.P.G. (2002), "Effectiveness of vertical drains in mitigation of liquefaction", *Soil Dyn. Earthq. Eng.*, **22**(9-12), 1059-1065. https://doi.org/10.1016/S0267-7261(02)00131-8.

Byrne, P.M. (1991), "A cyclic shear-volume coupling and pore pressure model for sand", *Proceedings of the 2nd International Conference on Recent Advances in Geotechnical Earthquake Engineering and Soil Dynamics*, St Louis, Missouri, U.S.A., April-May.

Castiglia, M., de Magistris, F.S. and Napolitano, A. (2018), "Stability of onshore pipelines in liquefied soils", *Geomech. Eng.*, **14**(4), 355-366. http://doi.org/10.12989/gae.2018.14.4.355.

Castiglia, M., De Magistris, F.S., Morgante, S. and Koseki, J. (2019), "Geogrids as a remedial measure for seismic-liquefaction induced uplift of onshore buried gas pipelines", *Proceedings of the National Conference of the Researchers of Geotechnical Engineering*, Lecco, Italy, July.

Castiglia, M., Morgante, S., Napolitano, A. and De Magistris, F.S. (2017), "Mitigation measures for the stability of pipelines in liquefiable soils", *J. Pipeline Eng.*, **16**(3), 115-139.

Chakraborty, D. and Kumar, J. (2013), "Stability of a long unsupported circular tunnel in soils with seismic forces", *Nat. Hazards*, **68**(2), 419-431. https://doi.org/10.1007/s11069-013-0633-y.

Chian, S.C. and Madabhushi, S.P.G. (2012), "Effect of buried depth and diameter on uplift of underground structures in liquefied soils", *Soil Dyn. Earthq. Eng.*, **41**, 181-190. https://doi.org/10.1016/j.soildyn.2012.05.020.

Chian, S.C. and Madabhushi, S.P.G. (2013), "Remediation against floatation of underground structure", *Ground Improv.*, **166**(3), 155-167. https://doi.org/10.1680/grim.11.00030.

Chian, S.C., Tokimatsu, K. and Madabhushi, S.P.G. (2014), "Soil liquefaction-induced uplift of underground structures: Physical and numerical modeling", *J. Geotech. Geoenviron. Eng.*, **140**(10), 04014057. https://doi.org/10.1061/(ASCE)GT.1943-5606.0001159.

Chou, H.S., Yang, C.Y., Hsieh, B.J. and Chang, S.S. (2001), "A study of liquefaction related damages on shield tunnels", *Tunn. Undergr. Sp. Tech.*, **16**(3), 185-193. https://doi.org/10.1016/S0886-7798(01)00057-8.

Chou, J.C., Kutter, B.L., Travasarou, T. and Chacko, J.M. (2011), "Centrifuge modeling of seismically induced uplift for the BART transbay tube", *J. Geotech. Geoenviron. Eng.*, **137**(8), 754-765. https://doi.org/10.1061/(ASCE)GT.1943-5606.0000489.

Dobry, R., Ladd, R.S., Yokel, F.Y., Chung, R.M. and Powell, D. (1988), *Prediction of Pore Water Pressure Buildup and Liquefaction of Sands during Earthquakes by Cyclic Strain Method*, *Building Science Series*, Washington, D.C., U.S.A.

Elgamal, A. W., Dobry, R., Parra, E. and Yang, Z. (1998), "Soil dilation and shear deformation during liquefaction", *Proceedings of the 4th International Conference on Case Histories in Geotechnical Engineering,* St. Louis, Missouri, U.S.A., March.

Emirler, B., Tolun, M. and Laman, M. (2016), "Experimental investigation of the uplift capacity of group anchor plates embedded in sand", *Geomech. Eng.*, **11**(5), 691-711. http://doi.org/10.12989/gae.2016.11.5.691.

Fabozzi, S., Licata, V., Autuori, S., Bilotta, E., Russo, G. and Silvestri, F. (2017), "Prediction of seismic behaviour of an underground railway station and a tunnel in Napoli (Italy)", *Undergr. Sp.*, **2**(2), 88-105. https://doi.org/10.1016/j.undsp.2017.03.005.

Fiegel, G.L. and Kutter, B.L. (1994), "A mechanics of liquefaction for layered soils", *J. Geotech. Eng.*, **120**(4), 737-755. https://doi.org/10.1061/(ASCE)0733-9410(1994)120:4(737).

Finn, W.D.L. (1981), "Liquefaction potential: Developments since 1976", *Proceedings of the 1st International Conference on Recent Advances in Geotechnical Earthquake Engineering and Soil Dynamics*, St. Louis, Missouri, U.S.A., April.

FLAC3D 5.0 (2012), Itasca Consulting Group, Minneapolis, Minnesota, U.S.A.

Foriero, A. and Ladanyi, B. (1994), "Pipe uplift resistance in frozen soil and comparison with measurements", *J. Cold Reg. Eng.*, **8**(3), 93-111. https://doi.org/10.1061/(ASCE)0887-381X(1994)8:3(93).

Gregor, T. and Shobayry, R. (2011), "Seismic analysis of large underground structures using FLAC 3D", *Proceedings of the 2nd International FLAC/DEM Symposium*, Melbourne, Australia, February.

Huange, X., Schweiger, H.F. and Huang, H. (2013), "Influence of deep excavations on nearby existing tunnels", *Int. J. Geomech.*, 170-180. https://doi.org/10.1061/(ASCE)GM.1943-5622.0000188.

Ishii, H., Funahara, H., Matsui, H. and Horikoshi, K. (2013), "Effectiveness of liquefaction countermeasures in the 2011 M = 9 gigantic earthquake, and an innovative soil improvement method", *Indian Geotech. J.*, **43**(2), 153-160. https://doi.org/10.1007/s40098-012-0027-1.

Itasca Consulting Group. (2012), *FLAC3D 5.0 Manual*, Itasca Consulting Group, Minneapolis, Minnesota, U.S.A.

Kammerer, A.M., Wu, J., Riemer, M.F., Pestana, J.M. and Seed, R.B. (2004), "Shear strain development in liquefiable soil under bi-directional loading condition", *Proceedings of the 13th World Conference on Earthquake Engineering*, Vancouver, Canada, August.

Kang, G.C., Tobita, T. and Iai, S. (2014), "Seismic simulation of liquefaction-induced uplift behavior of a hollow cylindrical structure buried in shallow ground", *Soil Dyn. Earthq. Eng.*, **64**, 85-94. https://doi.org/10.1016/j.soildyn.2014.05.006.

Koseki, J., Matsuo, O. and Koga, Y. (1997b), "Uplift behaviour of underground structures caused by liquefaction of surrounding soil during earthquake", *Soils Found.*, **37**(1), 97-108. https://doi.org/10.3208/sandf.37.97.

Koseki, J., Matsuo, O., Ninomiya, Y. and Yoshida, T. (1997a), "Uplift of sewer manholes during 1993 Kushiro-Oki earthquake", *Soils Found.*, **37**(1), 109-121. https://doi.org/10.3208/sandf.37.109.

Kulhawy, F.H. and Mayne, P.W. (1990), "Manual on estimating soil properties for foundation design", Report EL-6800, Electric Power Research Institute, Palo Alto, California, Cornell University, Ithaca, New York, U.S.A.,

Ling, H.I., Mohri, Y., Kawabata, T., Liu, H., Burke, C. and Sun, L. (2008), "Finite element analysis of pipe buried in saturated soil deposit subject to earthquake loading", *J. Earthq. Tsunami*, **2**(1), 1-17. https://doi.org/10.1142/S1793431108000244.

Ling, H.I., Sun, L., Liu, H., Kawabata, T. and Mohri, Y. (2003), "Centrifuge modeling of seismic behavior of large-diameter pipe in liquefiable soil", *J. Geotech. Geoenviron. Eng.*, **129**(12), 1092-1101. https://doi.org/10.1061/(ASCE)1090-0241(2003)129:12(1092).

Liu, H. (2012), "Three-dimensional analysis of underground tunnels in liquefiable soil subject to earthquake loading" *Proceedings of the GeoCongress 2012: State of the Art and Practice in Geotechnical Engineering*, Oakland, Califronia, U.S.A., March.

Liu, H. and Song, E. (2006), "Working mechanism of cutoff walls in reducing uplift of large underground structures induced by soil liquefaction", *Comput. Geotech.*, **33**(4-5), 209-221. https://doi.org/10.1016/j.compgeo.2006.07.002.

Lombardi, D. and Bhattacharya, S. (2016), "Evaluation of seismic performance of pile-supported models in liquefiable soil", *Earthq. Eng. Struct. Dyn.*, **45**(6), 1019-1038. https://doi.org/ 10.1002/eqe.2716.

Lysmer, J. and Kuhlemeyer, R.L. (1969), "Finite dynamic model for infinite media", *J. Eng. Mech. Div.*, **95**(4), 859-877.

Madabhushi, S.S.C. and Madabhushi, S.P.G. (2015), "Finite element analysis of floatation of rectangular tunnels following earthquake induced liquefaction", *Indian Geotech. J.*, **45**(3), 233-242. https://doi.org/10.1007/s40098-014-0133-3.

Mahdim, M. and Katebi, H. (2015), "Numerical modeling of uplift resistance of buried pipelines in sand, reinforced with geogrid and innovative grid-anchor system", *Geomech. Eng.*, **9**(6), 757-774. http://doi.org/10.12989/gae.2015.9.6.757.

Mahmoud, A.O., Hussien, M.N., Karray, M., Chekired, M., Bessette, C. and Jinga, L. (2020), "Mitigation of liquefaction-induced uplift of underground structures", *Comput. Geotech.*, **125**, 103663. https://doi.org/10.1016/j.compgeo.2020.103663.

Mele, L., Lirer, S. and Flora, A. (2019), "The effect of densification on Pieve di Cento sands in cyclic simple shear tests", *Proceedings of the National Conference of the Researchers of Geotechnical Engineering*, Lecco, Italy, July.

Mitsuji, K. (2008), "Numerical simulations for development of liquefaction countermeasures by use of partially saturated sand", *Proceedings of the 14th World Conference on Earthquake Engineering*, Beijing, China, October.

Miyajima, M., Yoshida, M. and Kitaura, M. (1992), "Small scale tests on countermeasures against liquefaction for pipelines using gravel drain system", *Proceedings of the 4th Japan-US Workshop on Earthquake Resistant Design of Lifeline Facilities and Countermeasures for Soil Liquefaction.* Honolulu, Hawaii, U.S.A., May

Modoni, G., Albano, M., Salvatore, E. and Koseki, J. (2018), "Effects of compaction on the seismic performance of embankments built with gravel", *Soil Dyn. Earthq. Eng.*, **106**, 231-242. https://doi.org/10.1016/j.soildyn.2018.01.005.

Modoni, G., Croce, P., Proia, R. and Spacagna, R.L. (2019), "Guidelines and codes for liquefaction mitigation by ground improvement", *Proceedings of the IABSE Symposium, Guimaraes 2019: Towards a Resilient Built Environment Risk and Asset Management*, Guimarães, Portugal, March.

Murty, C.V.R. and Malik, J.N. (2008), "Challenges of Low-to-Moderate Seismicity in India", *Electron. J. Struct. Eng.*, **8**, 77-87.

Nagy, N., Mohamed, M. and Boot, J.C. (2010), "Nonlinear numerical modelling for the effects of surface explosions on buried reinforced concrete structures", *Geomech. Eng.*, **2**(1), 1-18. http://doi.org/10.12989/gae.2010.2.1.001.

Nobahar, A., Kenny, S. and Phillips, R. (2007), "Buried pipelines

subjected to subgouge deformations", *Int. J. Geomech.*, **7**(3), 206-216. https://doi.org/10.1061/(ASCE)1532-3641(2007)7:3(206).

Olarte, J.C., Dashti, S., Liela, A.B. and Paramasivam, B. (2018), "Effects of drainage control on densification as a liquefaction mitigation technique", *Soil Dyn. Earthq. Eng.*, **110**, 212-231. https://doi.org/10.1016/j.soildyn.2018.03.018.

Onoue, A. and Toyota, H. (2008), "Damage induced by the 2007 Niigataken Chuetsu-Oki earthquake", *Proceedings of the 14th World Conference on Earthquake Engineering*, Beijing, China, October.

Orense, R.P., Morimoto, I., Yamamoto, Y., Yumiyama, T., Yamamoto, H. and Sugawara, K. (2003), "Study on wall-type gravel drains as liquefaction countermeasure for underground structures", *Soil Dyn. Earthq. Eng.*, **23**(1), 19-39. https://doi.org/10.1016/S0267-7261(02)00152-5.

Otsubo, M., Towhata, I., Hayashida, T., Liu, B. and Goto, S. (2016b), "Shaking table tests on liquefaction mitigation of embedded lifelines by backfilling with recycled materials." *Soils Found.*, **56**(3), 365-378. https://doi.org/10.1016/j.sandf.2016.04.004.

Otsubo, M., Towhata, I., Hayashida, T., Shimura, M., Uchimura, T., Liu, B., Taeseri, D., Cauvin, B. and Rattez, H. (2016a), "Shaking table tests on mitigation of liquefaction vulnerability for existing embedded lifelines", *Soils Found.*, **56**(3), 348-364. https://doi.org/10.1016/j.sandf.2016.04.003.

Paramasivam, B., Dashti, S. and Liel, A. (2018), "Influence of prefabricated vertical drains on the seismic performance of structuresfFounded on liquefiable soils", *J. Geotech. Geoenviron. Eng.*, **144**(10), 04018070. https://doi.org/10.1061/(ASCE)GT.1943-5606.0001950.

Rasouli, R., Towhata, I., Rattez, H. and Vonaesch, R. (2018), "Mitigation of non-uniform settlement of structures due to seismic liquefaction", *J. Geotech. Geoenviron. Eng.*, **144**(11), 04018079. https://doi.org/10.1061/(ASCE)GT.1943-5606.0001974.

Robert, D.J. and Thusyanthan, N.I. (2016), "Numerical and experimental study of uplift mobilization of buried pipelines in sands", *J. Pipelines Syst. Eng. Pract.*, **6**(1), 04014009. https://doi.org/10.1061/(ASCE)PS.1949-1204.0000179.

Robert, D.J., Soga, K. and O'Rourke, T.D. (2016), "Pipelines subjected to fault movement in dry and unsaturated soils", *Int. J. Geomech.*, **16**(5), C4016001. https://doi.org/10.1061/(ASCE)GM.1943-5622.0000548.

Seed, H.B. and Booker, J.R. (1976), "Stabilisation of potentially liquefiable sand deposit using gravel drain systems", Report No. EERC 76-10, University of California, Berkeley, California, U.S.A.

Sherson, A.K., Nayyerloo, M. and Horspool, N.A. (2015), "Seismic performance of underground pipes during the Canterbury earthquake sequence", *Proceedings of the 10th Pacific Conference on Earthquake Engineering*, Sydney, Australia, November.

Singh, K., Mittal, S. and Kumar, K. (2018), "Reduction in lateral displacement of cohensionless soil at box tunnel face using nails in overburden", *Int. J. Geosynth. Ground Eng.*, **4**(3), 21. https://doi.org/10.1007/s40891-018-0138-6.

Stringer, M. and Madabhushi, G. (2007), "Modelling of liquefaction around tunnels", *Proceedings of the 4th International Conference on Earthquake Geotechnical Engineering*, Thessaloniki, Greece, June.

Sudevan, P.B, Boominathan, A. and Banerjee, S. (2020), "Numerical study on the liquefaction-induced uplift of an underground structure", *Int. J. Geomech.*, **20**(2), 06019020. https://doi.org/10.1061/(ASCE)GM.1943-5622.0001578.

Sudevan, P.B., Boominathan, A. and Banerjee, S. (2018), "Uplift analysis of an underground structure in a liquefiable soil subjected to dynamic loading", *Proceedings of the Geotechnical Earthquake Engineering and Soil Dynamics V*, Austin, Texas, U.S.A., June.

Taeseri, D., Otsubo, M., Laue, J. and Towhata, I. (2016), "New mitigation method for pipeline uplift during seismic event", *Geotech. Res.*, **3**(2), 54-64. https://doi.org/10.1680/jgere.16.00002.

Tanaka, T., Yasuda, S., Ohtsuka, T. and Kanemaru, Y. (2011), "Uplift of sewage pipes during the 2007 Niigataken Chuetsu-Oki Earthquake", *Proceedings of the 5th International Conference on Earthquake Geotechnical Engineering*, Santiago, Chile, January.

Tanaka, Y., Komine, H., Tohma, J., Ohtomo, K. and Tochigi, H. (1995), "Area of compaction to prevent uplift by liquefaction", *Proceedings of the 3rd International Conference on Recent Advances in Geotechnical Earthquake Engineering and Soil Dynamics*, St. Louis, Missouri, U.S.A., April.

Tobita, T., Kang, G.C. and Lai, S. (2011), "Centrifuge modeling on manhole uplift in a liquefiable trench", *Soils Found.*, **51**(6), 1091-1102. https://doi.org/1091-1102.10.3208/sandf.51.1091.

Tokimatsu, K. and Katsumata, K. (2012), "Liquefaction-induced damage to building in Urayasu City during the 2011 Tohoku Pacific earthquake", *Proceedings of the International Symposium on Engineering Lessons Learned from the 2011 Great East Japan Earthquake*, Tokyo, Japan, March.

Wang, B., Zen, K., Chen, G.Q. and Kasama, K. (2012), "Effects of excess pore pressure dissipation on liquefaction-induced ground deformation in 1g-shaking table test", *Geomech. Eng.*, **4**(2), 91-103. http://doi.org/10.12989/gae.2012.4.2.091.

Watanabe, K., Sawada, R. and Koseki, J. (2016), "Uplift mechanism of open-cut tunnel in liquefied ground and simplified method to evaluate the stability against uplifting", *Soils Found.*, **56**(3), 412-426. https://doi.org/10.1016/j.sandf.2016.04.008.

Wu, J., Kammerer, A.M., Riemer, M.F., Seed, R.B. and Pestana, J.M. (2004), "Laboratory study of liquefaction triggering criteria", *Proceedings of the 13th World Conference on Earthquake Engineering*, Vancouver, Canada, August.

Yang, D., Naesgaard, E., Byrne, P.M., Adalier, K. and Abdoun, T. (2004), "Numerical model verification and calibration of George Massey tunnel using centrifuge models", *Can. Geotech. J.*, **41**(5), 921-942. https://doi.org/10.1139/t04-039.

Yang, J. and Wang, H.D. (2012), "Seismic response analysis of shallow utility tunnel in liquefiable soils", *Proceedings of the International Conference on Pipelines and Trenchless Technology*, Wuhan, China, October.

Yasuda, S. and Kiku, H. (2006), "Uplift of sewage manholes and pipes during the 2004 Niigataken-Chustsu earthquake", *Soils Found.*, **46**(6), 885-894. https://doi.org/10.3208/sandf.46.885.

Yatsumoto, H., Mitsuyoshi, Y., Sawamura, Y. and Kimura, M. (2019), "Evaluation of seismic behavior of box culvert buried in the ground through centrifuge model tests and numerical analysis", *Undergr. Sp.*, **4**(2), 147-167. https://doi.org/10.1016/j.undsp.2018.09.007.

Yegian, M.K., Eseller-Bayat, E., Alshawabkeh, A. and Ali, S. (2007), "Induced-partial saturation for liquefaction mitigation: Experimental investigation", *J. Geotech. Geoenviron. Eng.*, **133**(4), 372-380. https://doi.org/10.1061/(ASCE)1090-0241(2007)133:4(372).

Yigit, A., Lav, M.A. and Gedikli, A. (2018), "Vulnerability of natural gas pipelines under earthquake effects", *J. Pipelines Syst. Eng. Pract.*, **9**(1), 04017036. https://doi.org/10.1061/(ASCE)PS.1949-1204.0000295.

Yoshimi, Y. (1998), "Simplified design of structures buried in liquefiable soil", *Soils Found.*, **38**(1), 235-240. https://doi.org/10.3208/sandf.38.235.

Yu, H., Yuan, Y. and Bobet, A. (2017), "Seismic analysis of long

tunnels: A review of simplified and unified methods", *Undergr. Sp.*, **2**(2), 73-87. https://doi.org/10.1016/j.undsp.2017.05.003.

JS